Anion exchange membranes derived from poly(ionic liquid) of poly(bis-piperidinium) and polybenzimidazole blends

Zhao, Beijia; Wang, Tingting; Kraglund, Mikkel Rykær; Yang, Jing; Dong, Jianhao; Tang, Ao; Aili, David; Yang, Jingshuai

Published in:
Journal of Molecular Liquids

Link to article, DOI:
10.1016/j.molliq.2024.124775

Publication date:
2024

Document Version
Publisher's PDF, also known as Version of record

Journal of Molecular Liquids 402 (2024) 124775

Contents lists available at ScienceDirect

Journal of Molecular Liquids

journal homepage: www.elsevier.com/locate/molliq

Anion exchange membranes derived from poly(ionic liquid) of poly (bis-piperidinium) and polybenzimidazole blends

Beijia Zhao [a], Tingting Wang [a], Mikkel Rykær Kraglund [b], Jing Yang [c], Jianhao Dong [a], Ao Tang [c,*], David Aili [b,*], Jingshuai Yang [a,*]

[a] Department of Chemistry, College of Sciences, Northeastern University, Shenyang 110819, China
[b] Department of Energy Conversion and Storage, Technical University of Denmark, Elektrovej Building 375, 2800 Lyngby, Denmark
[c] Institute of Metal Research, Chinese Academy of Sciences, Shenyang 110016, China

ARTICLE INFO

Keywords:
Ether-free anion exchange membrane
Main-chain bis-piperidinium
Blending
Polybenzimidazole
Poly(ionic liquid)

ABSTRACT

Anion exchange membranes (AEMs) play a critical role in various environmentally friendly electrochemical energy conversion and storage devices such fuel cells, water electrolysis and flow batteries. Recently, AEMs based on ether-free ionomers or ionenes have attracted much attention due to their excellent alkaline stabilities, however normally suffering from multiple-step synthetic procedure, post-functionalization and the use of precious metal catalysts. In this study, we develop a facile method to synthesize bis-piperidinium main-chain poly(ionic liquid)s devoid of ether linkages through the nucleophilic reaction between a bis-piperidine monomer of 4,4′-trimethylene bis(1-methyl-piperidine) and various bifunctional alkyl or aryl bromides. Seven poly(ionic liquid)s of poly(bis-alkyl piperidinium) are subsequently blended with polybenzimidazole (PBI) to give mechanically robust and dimensionally stable AEMs. The membrane performances are readily adjusted by changing the chemical structure of poly(bis-alkyl piperidinium)s. The membrane based on the poly(bis-alkyl piperidinium) containing a flexible butylidene spacer chain achieves the highest Br^- conductivity of 67 mS cm^{-1} at 80 °C, tensile strength of around 13 MPa at room temperature, and a superior alkaline stability in 1 mol/L KOH at 60 °C during 1250 h. Density functional theory calculations further support the enhanced alkaline stability of the piperidinium cation with alkyl group compared with the one with benzyl group.

1. Introduction

Recently anion exchange membranes (AEMs) have obtained tremendous attention due to the significant advantages when implementing them in fuel cells [1–3], water electrolysis [4–6], flow batteries [7,8] and other environmentally friendly electrochemical energy conversion and storage devices [9,10]. One of the most important functions of AEMs is to support the current between the electrodes, while high OH^- conductivity is needed to suppress ohmic resistance. In addition, the AEM should prevent crossover of reactants and products, possess good dimensional and mechanical stabilities, and superior alkaline tolerance under high-pH and high temperature conditions [2,4,11]. Although significant efforts have been done to enhance performances of AEMs over the past decade, the alkaline stability of AEMs is also under challenge.

The alkaline stability of AEMs is related primarily to the cationic groups and the grafted side chains, but also to the polymer backbones. Most AEMs are based on quaternary ammonium (QA) cation-functionalized polyarylenes [12–15]. A common method to introduce QA group is the functionalization of commercially available poly(arylene ether)s such as poly(phenylene oxide) [16,17,18,19], poly(arylene ether ketone) [20,21,22] and poly(arylene ether sulfone) [23,24] via chloromethylation or bromomethylation followed by quaternization. However, the benzylic QA groups degrade easily in strong alkaline environments, mainly owing to S_N2 type substitution and E1 elimination pathways [12,25–27]. It has recently been reported that the introduction of alternative *N*-heterocyclic cations, such as imidazolium [16,28,29], pyrrolidinium [30–32] and piperidinium [33–35] effectively mitigate common degradation reactions. On the other hand, the linkers and polymer backbones of AEMs should also be carefully designed. Marino et al. [12] and Kim et al. [36] independently observed that the QA in benzylic position rapidly degrade by substitution because of the electron-withdrawing inductive influence of the aromatic group, which makes the benzylic carbon much easier to be attacked by OH^-

* Corresponding authors.
E-mail addresses: a.tang@imr.ac.cn (A. Tang), larda@dtu.dk (D. Aili), yjs@mail.neu.edu.cn (J. Yang).

https://doi.org/10.1016/j.molliq.2024.124775
Received 11 February 2023; Received in revised form 3 April 2024; Accepted 17 April 2024
Available online 18 April 2024

[26,27]. Meanwhile, benzylic cations have been proven to destabilize arylene-ether bonds of the polymer main chain, especially in the presence of other strongly electron-withdrawing structural elements such as sulfone linkages [36–38]. Hence, polymers devoid of arylene ether linkages have received increasing attention in recent years, such as polyfluorenes [39], poly(vinyl benzyl chloride) (PVBC) [31,40], polystyrene-*b*-poly(ethylene-*co*-butylene)-*b*-polystyrene (SEBS) [32,41,42] and poly(olefin)s [43]. In addition, Yoo et al. adopted chemical crosslinking to improve the alkaline stability of AEMs [18,19,22]. Nevertheless, AEMs with cations in benzylic position still suffered from several disadvantages such as the usage of toxic chemicals during halomethylation and difficulty in controlling the grafting degree and eliminating side reactions [13].

As an attractive strategy, ether-free and main-chain cation type AEMs have been widely developed recently, such as imidazolium [44–47], piperidinium [48–50] and pyrrolidinium [51] main-chain cation based AEMs. For example, Fan et al. synthesized poly(arylene-imidazolium) ionenes with sterically bulky groups in the imidazolium C2 position [45], which exhibited good alkaline stability in 10 mol/L KOH at 100 °C in the form of membranes. Pham et al. synthesized piperidinium main-chain AEMs based on *N*-spirocyclic QA ionenes through cyclo polycondensation [48]. However, the synthesis of those high-performance membranes need multiple-step synthetic procedure, post-functionalization and precious metal catalysts [35]. Thus, developing facile methods to synthesize high-performance ether-free ionenes that combine alkaline stability with high ion conductivity is still a challenge. Recently, ionic liquids have been used in AEMs due to their high ionic conductivity, excellent chemical stability and thermal stability. Yan et al. [51] and Guo et al. [52] reported the preparation of AEMs based on imidazolium and pyrrolidinium-type ionic liquids. Especially, poly(ionic liquid)s combine the merits and avoid the problems of ionic liquids, which have attracted more and more attentions in the field of AEMs [53,54].

In our previous work, we have developed an operationally simple methodology to synthesize bis-imidazolium poly(ionic liquid)s via the nucleophilic substitution between bis-imidazoles and bifunctional alkyl/benzyl bromides [29,55]. Although the poly(bis-alkyl imidazolium) poly(ionic liquid)s displayed high conductivity, their alkaline stability, especially in basic solutions with high concentrations, remained to be improved. In this study, the structural scope of the ether-free bis-piperidinium main-chain poly(ionic liquid)s is extended by polymerizing a bispiperidine monomer with a series of bifunctional alkyl/benzyl bromide monomers. This synthesis route possessed several advantages for cation main-chain AEMs, including (a) straightforward one-step synthesis without side reactions, (b) metal catalyst free conditions, and (c) wide structural scope. Meanwhile the content and location of the cationic group was precisely adjusted, and post modification was not required. Due to the presence of piperidinium cations in the backbone, the resulting poly(ionic liquid)s exhibited significant hydrophilicity and swelling in water. The poly(ionic liquid)s were therefore blended with polybenzimidazole (PBI) to balance the swelling and to obtain mechanically robust and stable AEMs.

2. Experimental

2.1. Materials

1,2-Dibromoethane (C_2), 1,4-dibromobutane (C_4), 1,6-dibromohexane (C_6), 1,8-dibromooctane (C_8), 1,10-dibromodecane (C_{10}), 1,12-dibromododecane (C_{12}) and α, α'-dibromo-*p*-xylene (C_{Bn}) were purchased from Adamas-beta. 4,4′-Trimethylenebis(1-methyl-piperdine) (TMBMP) was bought from Sigma-Aldrich. Dimethyl sulfoxide (DMSO), *N*,*N*-dimethylformamide (DMF), acetone and other chemicals were bought from Tianjin Fuyu Chemical Co., Ltd. China. Poly(2,2′-(*m*-phenylene)-5,5′-bibenzimidazole)) (PBI) with an inherent viscosity of 0.98 dL g^{-1} was synthesized based on our previous work [56].

2.2. Poly(bis-piperidinium) synthesis and membrane fabrication

As illustrated in Fig. 1, the poly(ionic liquid)s of poly(bis-piperidinium) bromides were synthesized by dissolving the bis-bromo monomers (1.74–3.04 g, 9.26 mmol) and TMBMP (2.21 g, 9.26 mmol) in 70 mL DMF and 10 mL DMSO. The mixture was stirred at 80 °C under N_2 atmosphere for 24 h, and the formed polymer was thereafter precipitated in acetone and washed three times with acetone. However, the polymer from dibromoethane and TMBMP did not precipitate by pouring the crude into acetone, and was instead isolated by evaporating the DMF/DMSO mixture under reduced pressure. The residue was thereafter washed with acetone, and a dark red liquid was obtained by evaporating the acetone under reduced pressure. The poly(bis-piperidinium) poly(ionic liquid)s are hereafter named Pip-C_x, where *x* refers to the bis-bromo monomer (i.e. 2, 4, 6, 8, 10, 12 and Bn) according to the nomenclature defined in section 3.1.

The poly(bis-piperidinium) poly(ionic liquid)s and PBI blend membranes were fabricated by a solution-casting method as shown in Fig. 1. Ether Pip-C_x oligomer or PBI polymer was added into DMSO to prepare a homogenous solution, and the concentration was around 3 wt%. Then Pip-C_x and PBI solutions with a molar ratio of 2:1 (Pip-C_x to PBI) were mixed at room temperature (RT), followed by ultrasonication for 1 h. The obtained solution was cast onto a clean Petri dish (diameter: 6.5 cm) and evaporated at 80 °C for 2 days. The resulting membranes were washed in deionized water, and hereafter referred to as Pip-C_x/PBI. Finally, AEMs in form of OH^- were obtained by immersing membranes in 1 mol/L KOH at RT for 3 days, followed by washing in deionized water to remove the excess KOH.

2.3. Characterizations

The inherent viscosity (η_{inh}) was measured with an Ubbelohde viscometer at 25 °C in DMSO using a polymer concentration of 50 mg dL^{-1}. Then η_{inh} was calculated according to Eq. (1), where t_s is the efflux time of the polymer solution, t_b is the outflow time of the pure DMSO, and c is the concentration.

$$\eta\left(dL{\cdot}g^{-1}\right) = \ln(t_s/t_b)/c \tag{1}$$

The ^{1}H NMR spectra of polymers were obtained on the Bruker AVANCE 600 MHz instrument using deuterium oxide (D_2O) as the solvent. The water absorption and swelling were measured based on the variations of mass, volume, or area before (*B*) and after (*A*) water absorption at different temperatures according to Eq. (2).

$$Value\,(\%) = (A - B)/B \times 100 \tag{2}$$

According to back titration, the ion exchange capacity (IEC) of membranes was determined. The membranes in the OH^- form were cut into pieces and soaked in 0.05 mol/L HCl (aq.) for 2 days at RT, and the HCl solution was thereafter titrated with aqueous KOH (0.1 mol/L) followed with a pH meter. The IEC of the membranes was determined based on Eq. (3), and V_1 and V_2 are the volumes of the standard KOH solution for the blank and membrane samples, and *m* is the dry weight of the polymer.

$$IEC\left(mmol\,g^{-1}\right) = (V_1 - V_2) \times c_{KOH} \times 10^3/m \tag{3}$$

Thermogravimetric analysis (TGA) was performed in N_2 at a heating rate of 10 °C min^{-1} and tested by a Mettler Toledo TGA/DSC^{3+} from 30 to 800 °C. The hydrated membrane sample was processed into a dumbbell shape having an area of 4 mm × 25 mm, and the stress-strain curves were recorded using a CMT6502 (SANS, China). The conductivity was determined in the bromide (Br^-) form in pure water (Wahaha Pure Water with a conductivity of about 2 μS cm^{-1}). After recording the length and cross-sectional area of the sample, the conductivity was measured in the plane of the membrane by electrochemical impedance spectroscopy (Princeton VersaSTAT 3) using a two-electrode cell in a

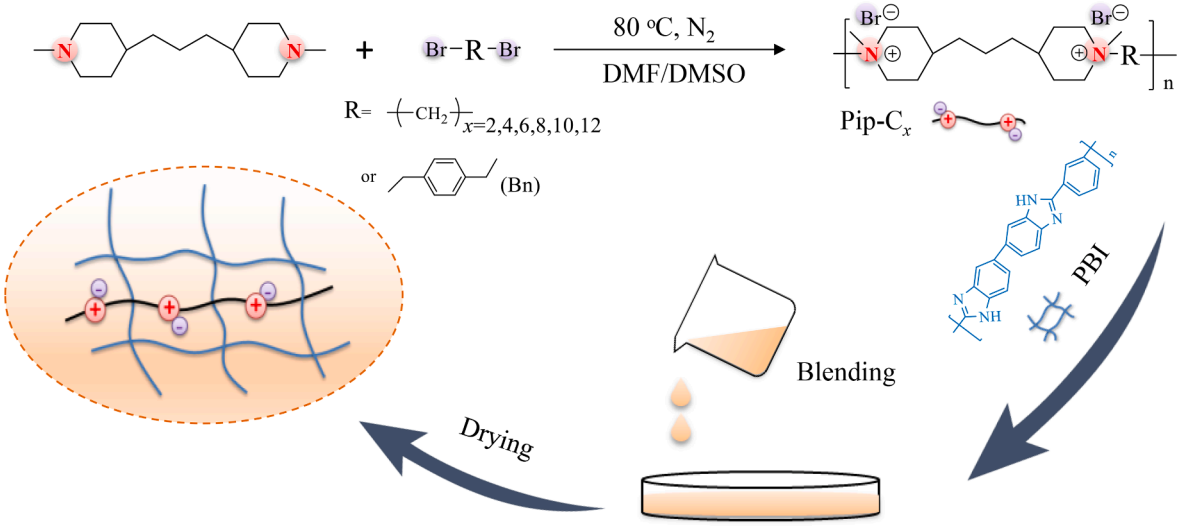

Fig. 1. Scheme of poly(bis-piperidinium) synthesis and membrane fabrication.

water bath at different temperature. At the AC frequency from 0.1 Hz to 100 kHz, the ohmic resistance was taken as the real part of the impedance. The conductivity of the membranes was calculated by Eq. (4), and L (cm), S (cm^2), and R (Ω) represent the length, cross-sectional area and resistance, respectively.

$$\sigma\left(S{\cdot}cm^{-1}\right) = L/(R \times S) \tag{4}$$

The alkali resistance measurement was carried out by immersing the membranes in 1 or 8 mol/L KOH solution at 80 °C and monitored by the changes in conductivity (in form of Br^-), IEC, and mechanical strength over time. At the same time, the polymer was dissolved in 1 mol/L NaOD solution at 80 °C to observe the ^{1}H NMR peak change of the polymer at different time.

2.4. DFT calculations

Density functional theory (DFT) calculations were carried out using Gaussian 09 based on B3LYP, where the all structures were firstly optimized with 6-31G (d,p) basis set and subsequently refined with 6–311 + G (d,p) basis set, together with tight convergence criteria and no symmetry. Both reactants and products were optimized to an energy minimum, and transition states (TS) search were conducted using Berny algorithm and confirmed by calculating the intrinsic reaction coordinate (IRC). Frequency analysis at 298.15 K was performed to obtain both reaction free energy activation energy.

3. Results and discussion

3.1. Synthesis of Pip-C_x poly(ionic liquid)s and fabrication of membranes

A series of poly(bis-piperidinium)s (i.e., Pip-C_x poly(ionic liquid)s) was defined and synthesized through the facile nucleophilic substitution polymerization between TMBMP and the bifunctional alkyl (or benzyl) bromides of different length, as illustrated in Fig. 1. This chemical concept has previously been adopted for preparing AEMs, including *N*-spirocyclic iononenes [48] and imidazolium poly(ionic liquid)s [55]. Fig. 2 shows the inherent viscosities of the different Pip-C_x poly(ionic liquid)s. When increasing the length of the aliphatic chain, the inherent viscosity was correspondingly increased. Among them, the inherent viscosity of Pip-C_2 was only 0.17 dL g^{-1}, but the inherent viscosity of Pip-C_{12} derived from 1,12-dibromododecane was as high as 0.51 dL g^{-1}. Furthermore, because of the high reactivity of α, α'-dibromo-*p*-xylene, the inherent viscosity of Pip-C_{Bn} reached the highest value of 0.61 dL g^{-1}.

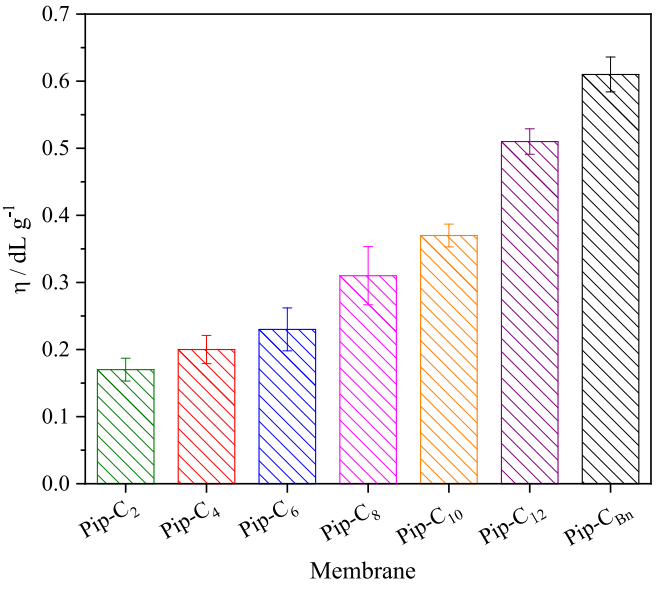

Fig. 2. Inherent viscosity of the different poly(bis-piperidinium)s.

The structural identity of the obtained polymers and the Pip monomer was determined by ^{1}H NMR as depicted in Fig. 3 and Fig. S1 (Supporting Information). Comparing with the ^{1}H NMR result of Pip, Pip-C_x polymers displayed obviously different characteristic peaks. Taking an example of the Pip-C_{Bn} polymer from α, α'-dibromo-*p*-xylene and TMBMP (Fig. 3g), the existing peak at 4.6 ppm can be assigned to the methylene group connecting the benzene ring and piperidinium unit [35,55,57], while the peak due to the benzene ring appears at 7.68 ppm. The peak at 3.45 ppm is assigned to the methylene group adjacent to the spirocyclic *N*-position of the bis-piperidinium cations, and the peak of the methyl group appears at 3.01 ppm [35,48]. In summary, the appearance of these peaks supports the successful synthesis of Pip-C_{Bn}. For other Pip-C_x poly(ionic liquid)s synthesized from fully aliphatic monomers (Fig. 3a–f), the peaks are mainly concentrated between 1.0–4.0 ppm. The characteristic peaks at 2.9 to 3.6 ppm correspond to the methyl and methylene groups adjacent to the spirocyclic *N*-position of piperidinium moieties. The methylene peaks further away from the electron withdrawing piperidinium cations all appear between 1.0 and 2.0 ppm, supporting the aliphatic structure as expected. In addition, the

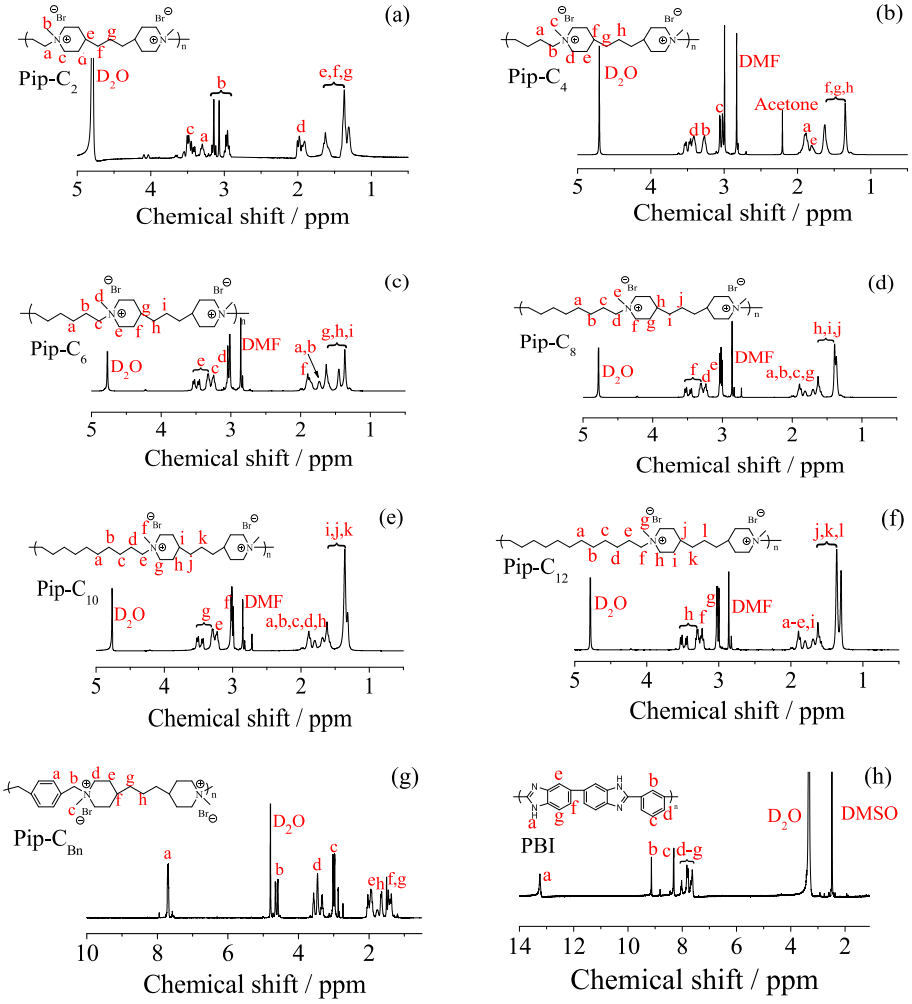

Fig. 3. ^{1}H NMR spectra of various Pip-C$_x$ poly(ionic liquid)s and PBI polymer.

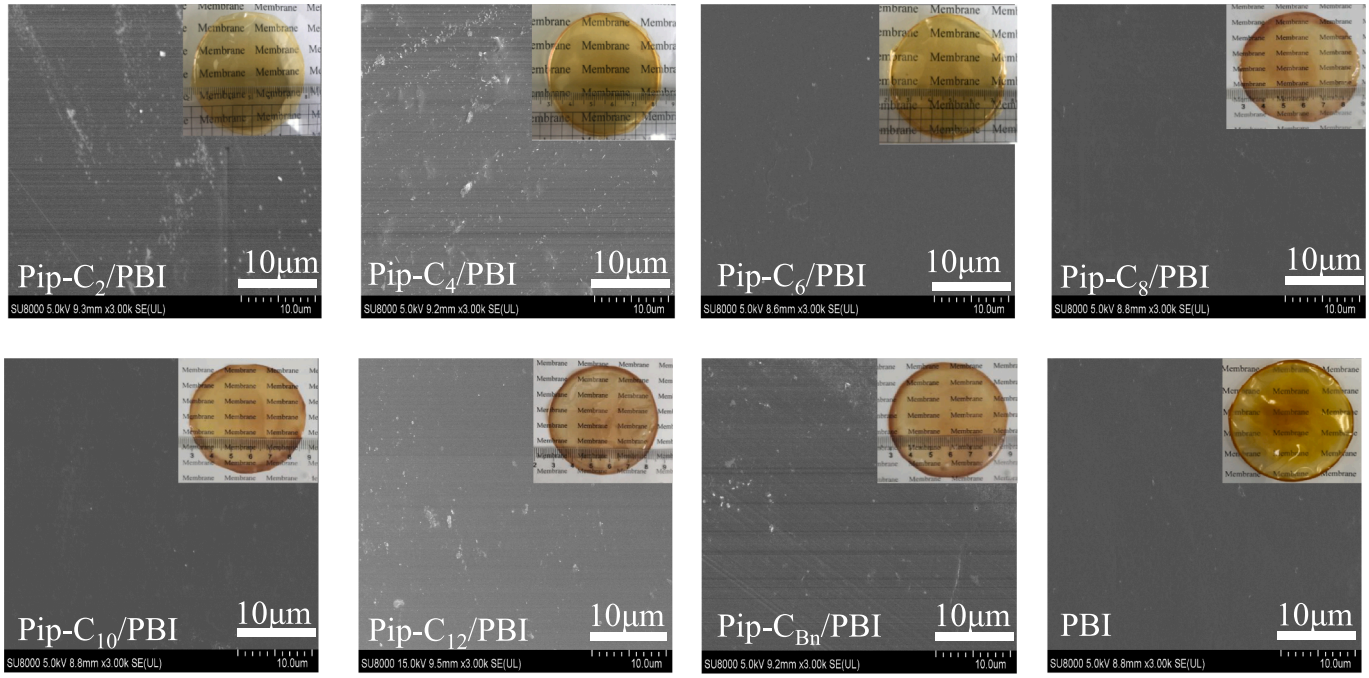

Fig. 4. Photos and surface SEM images of Pip-C$_x$/PBI blend membranes.

^{1}H NMR spectrum of PBI is shown in Fig. 3h, whose characteristic peaks are assigned in previous work [58].

Due to hydrophilicity and relatively low molecular weight of the pristine Pip-C_x poly(ionic liquid)s, PBI blending was adopted in order to obtain mechanically robust and water-insoluble membranes [29,48,55]. As pointed out by Pham et al. [48], the intermolecular interaction between the *N*-spirocyclic structure and benzimidazole unit in PBI contributed to the stabilization of the blend membrane in the alkaline environment. Thus, a series of Pip-C_x/PBI blend membranes were fabricated by the solution co-casting approach. Golden-yellow, transparent and uniform membranes were obtained as shown in Fig. 4. Meanwhile, SEM images in Fig. 4 demonstrate that all the obtained blend Pip-C_x/PBI membranes appeared uniform and dense at the micrometer length scale.

3.2. IEC, water uptake and swellings

Table 1 lists the measured and theoretical IEC values of different Pip-C_x/PBI membrane. The theoretical IEC values were obtained based on the chemical structures and compositions of the blend membranes. It is shows that the theoretical IEC decreased by increasing the length of the alkyl chain, mainly resulting from the increased repeat unit molecular weight of the poly(ionic liquid)s with a longer alkyl chain. For instance, the IEC of the Pip-C_2/PBI blend membrane was about 1.53 mmol g^{-1}, while that of the Pip-C_{12}/PBI membrane was decreased to 1.01 mmol g^{-1}. Meanwhile, the titrated IEC was lower than the theoretical value for all membranes, possibly resulting from the partial ion exchange. Similar phenomenon has been reported in previous works [3,30].

Water absorption is critical for AEMs to dissociate and solvate the ionic species in the membrane, and thus water molecules are involved in the hydroxide conduction [11,13]. The increase in concentration of ionic groups in an AEM generally raises water uptake, which facilitates ion mobility and enhances ionic conductivity until a point where dilution effects take over. However, the mechanical performance of the membrane will deteriorate due to excessive water uptake and swelling. Therefore, the water uptake need to be carefully balanced to obtain optimal properties. Fig. 5a shows the water uptake of various membrane samples at a range of temperatures. At each temperature, the Pip-C_{Bn}/PBI membrane reached the highest water uptake value. For example, the water uptake reached 138 % at 30 °C, which may be related to a relatively high free volume [11,42]. As to other fully aliphatic main-chain Pip-C_x/PBI membranes, the water uptake was found to increase by increasing the length of the alkyl chain. As a result, the Pip-C_{12}/PBI membrane reached a high water uptake of 81 % at 30 °C, while the Pip-C_2/PBI membrane exhibited a water uptake value of 26 % under the same testing condition. This might be related to the fact that the longer alkyl chain might provide a larger free volume for water absorption.

Meanwhile, Fig. 5a shows that the temperature had little effect on the water uptake, and the water uptake remained nearly constant at 30–80 °C. For example, the water uptake was 47 % and 50 % for the Pip-C_4/PBI membrane at 30 °C and 80 °C. As depicted in Fig. 5b and c, the area and volume swellings displayed a similar water uptake trend with increasing temperature. All membranes showed almost unchanged area or volume swelling as the temperature was raised from 30 °C to 80 °C.

Table 1
Theoretical and titrated IEC values (mmol g^{-1}) of Pip-C_x/PBI membranes.

Membrane	Pip-C_2/PBI	Pip-C_4/PBI	Pip-C_6/PBI	Pip-C_8/PBI	Pip-C_{10}/PBI	Pip-C_{12}/PBI	Pip-C_{Bn}/PBI
Theoretical[a]	1.53	1.47	1.19	1.04	1.06	1.01	1.36
Titrated	1.38 ± 0.15	1.19 ± 0.12	1.08 ± 0.13	1.06 ± 0.12	0.89 ± 0.17	0.91 ± 0.17	1.15 ± 0.12

[a] Calculated based on the chemical structures shown in Fig. 3 and the blend composition.

Among all the membranes, the Pip-C_{Bn}/PBI membrane displayed the largest area and volume swellings at each temperature, obviously resulting from its quite high water uptake. As to the fully aliphatic main-chain Pip-C_x/PBI membranes, the membrane displayed first decreased and then increased swelling when the length of the aliphatic carbon chain increased from 2 to 12 carbon atoms. This is probably due to the trade-off between free volume and water uptake. As the length of the aliphatic segments increased, both free volume and water uptake increased. The former factor might decrease swelling, while the latter parameter could increase swelling. Consequently, the Pip-C_6/PBI membrane possessed the lowest area and volume swellings at each temperature.

3.3. Conductivity and mechanical properties

Ionic conductivity is one of the key characteristics of AEMs in electrochemical systems, and high ion conductivity is essential to minimize the ohmic resistance of membrane electrode assemblies [2,10]. Recent work by Dekel's group [59] and by Holdcroft's group [60] show that carbonation when AEMs exposed to air is quick. In order to obtain accurate conductivity results, the conductivity of the different Pip-C_x/PBI blend membranes in the form of Br^- was measured and depicted in Fig. 6a. As to different Pip-C_x/PBI membranes, the membrane with a longer alkyl chain exhibited higher water uptake but lower IEC as discussed in above section. As a result of the combined effect of water absorption and IEC on ionic conductivity, the Pip-C_4/PBI membrane in the Br^- form exhibited the highest conductivity among all the membranes, reaching 67 mS cm^{-1} at 80 °C. However, the Pip-C_{12}/PBI membrane displayed the lowest conductivity among the membranes tested, although it had the highest water uptake (except Pip-C_{Bn}/PBI). Meanwhile, when the water uptake increased to a certain level, the dilution of conductive species resulted in decreased conductivity. It has previously been reported that methyl quaternized membrane (PTPipQ1) with a higher WU% value of 145 % showed a lower hydroxide conductivity than the corresponding hexyl quaternized membrane (PTPipQ6) with a WU% of 44 % at the same temperature [49]. Furthermore, the activation energy (E_a) of Pip-C*x*/PBI blend membranes were calculated according to following Equation: $\ln\sigma = \ln\sigma_0 - E_a/RT$ as previously reported by Yoo et al. [18]. As seen from Fig. S2, E_a values varied between 4.7 kJ mol^{-1} and 7.1 kJ mol^{-1}. Those values were lower or similar to those reported in previous works [19,21,30,40,42], implying a complex interplay of transport phenomena, potentially encompassing diffusion, migration, convection, and the Grotthuss mechanism. In addition, it should be noted that the conductivity of each membrane can be increased by exchanging the Br^- to OH^-, mainly due to the Grotthuss type structure diffusion contribution and intrinsically higher conductivity of OH^- than Br^- [59,61].

Excellent mechanical properties of AEM are required for the long-term durability of electrochemical energy conversion and storage devices [2,31]. The tensile strength and elongation at break of the blend membranes in Br^- form are summarized in Fig. 6b. Even though the Pip-C_{Bn}/PBI membrane showed the highest water uptake, it also had the highest tensile strength of 24 MPa among the membranes, mainly due to the high viscosity of the Pip-C_{Bn} component. As to the aliphatic main-chain membranes, it was found that the mechanical stability of the blend membranes were related to both water absorption and the viscosity of the poly(bis-piperidinium) used for the membrane fabrication. Since the increased viscosity represents an increase in molecular weight, the tensile strength of the blend membrane should increase accordingly [15,56]. However, the tensile strengths of Pip-C_{10}/PBI and Pip-C_{12}/PBI membranes were only around 8 MPa and 10 MPa, respectively. The low tensile strengths of above membranes might be related to the excessive water absorption, resulting in significant swellings and reduced mechanical strengths. Thus, the Pip-C_4/PBI and Pip-C_6/PBI membranes respectively represented tensile strengths of around 13 and 15 MPa, mainly owing to their low swellings. In addition, when increasing the

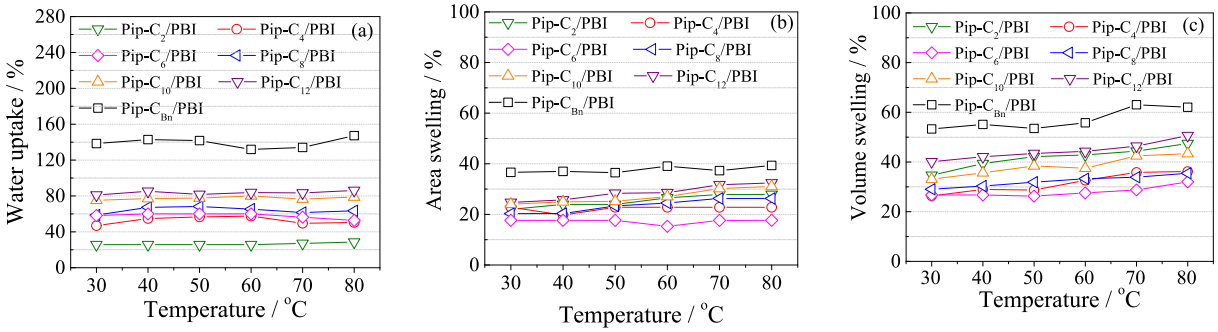

Fig. 5. Water uptake (a), area swelling (b) and volume swelling (c) of Pip-C$_x$/PBI membranes as a function of temperature.

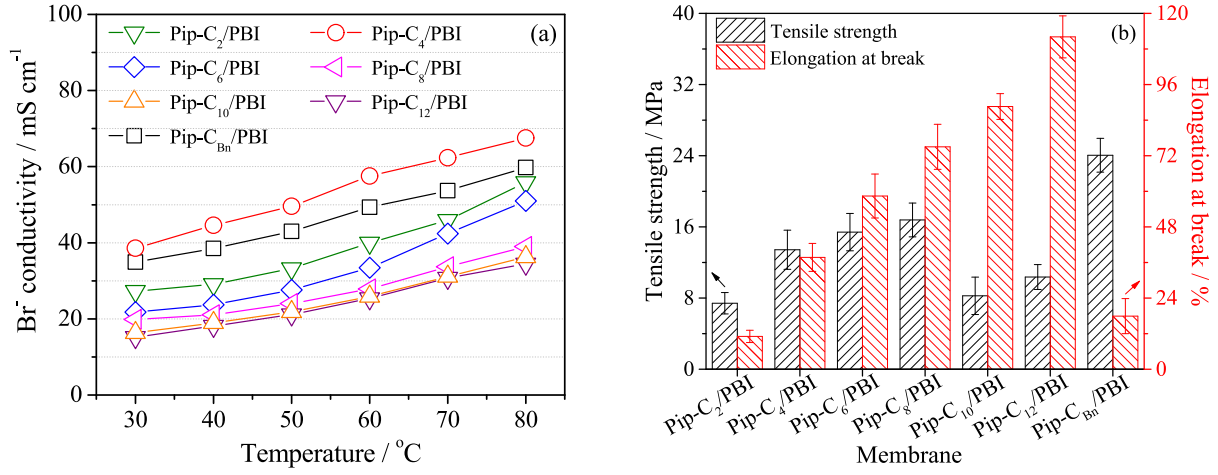

Fig. 6. (a) Conductivity of different membranes in the form of Br$^-$ as a function of temperature; (b) mechanical properties at RT.

length of the alkyl chain, the elongation at break generally increased. For example, the elongation at break of the Pip-C$_{12}$/PBI membrane was around 37 %, while that of the Pip-C$_2$/PBI membrane was as low as 4 %. It should be noted that the increase in elongation is often accompanied by a loss of tensile strength. Therefore, the trade-off needs be accounted for in order to obtain the optimum mechanical properties.

3.4. Thermal and alkaline stabilities

The cationic functional groups of AEMs are susceptible to hydroxide attack and undergo different degradation modes in alkaline environment, resulting in conductivity decay [11,12]. Therefore, it is necessary to study the alkaline stability of AEMs. Herein, simultaneously considering mechanical properties and conductivity results, the Pip-C$_4$/PBI, Pip-C$_6$/PBI and Pip-C$_{Bn}$/PBI membranes were chosen for thermal stability and alkaline stability experiments by submersing membranes in 1 mol/L KOH solution at 80 °C. Fig. 7 shows TGA curves of various membranes in N_2 at a heating rate of 10 °C min^{-1}. It is well known that the pure PBI membrane exhibits a quite high thermal stability below 500 °C [56]. As to Pip-Cx/PBI membranes, their mass loss below 150 °C mainly resulted from the evaporation of the water [29,55], followed by an onset of major degradation at around 300 °C.

Fig. 8 summarizes the Br$^-$ conductivity at 80 °C, IEC and tensile strength at RT of the three membranes after different testing time. After 1250 h, the conductivity of the three membranes was almost unchanged, indicating the superior alkali resilience of main-chain poly(bis-piperidinium)s. Similarly, Fig. 8b shows that IECs of the three membranes were almost unchanged after 1250 h, which also verified that the membranes had good alkaline stabilities. In addition, Fig. 8c shows the change of the tensile strength of membranes. The tensile strengths of the Pip-C$_4$/PBI and Pip-C$_6$/PBI membranes did not change significantly

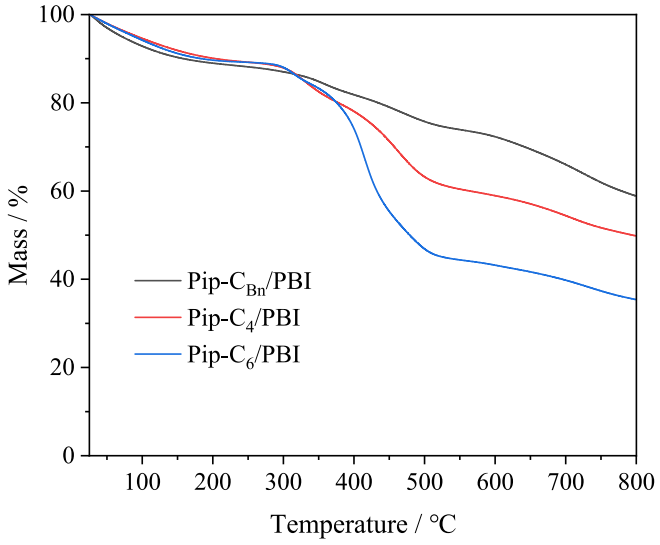

Fig. 7. TGA curves of various membranes in N_2 at a heating rate of 10 °C min^{-1}.

during the test, but the mechanical strength of the Pip-C$_{Bn}$/PBI membrane showed a slight decrease. As well-described in literature [26], AEMs are vulnerable to the hydroxide attack when the cationic functions are installed in benzylic position. These results indicate that Pip-C$_4$/PBI and Pip-C$_6$/PBI membranes showed excellent alkaline stabilities, which were comparable to other ether free AEMs. For example, after being immersed in 1 M KOH solution at 80 °C for 600 h, the FPAE-3B-3.0-PD

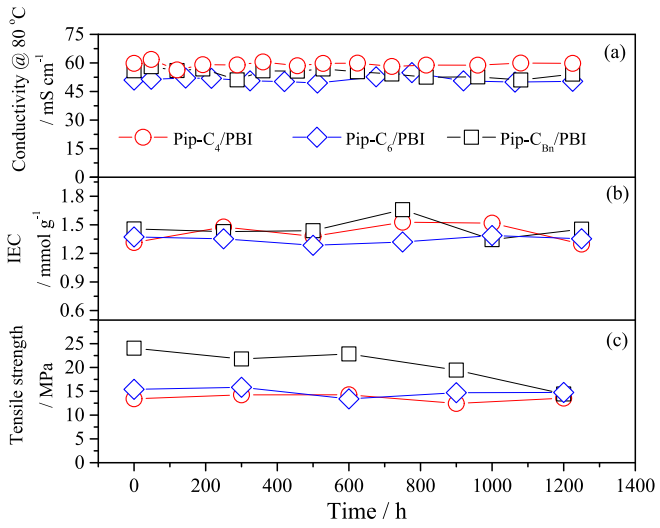

Fig. 8. Br^- conductivity at 80 °C (a), IEC (b) and tensile strength at RT (c) of various membranes immersing in 1 mol/L KOH at 80 °C as a function of time.

membrane retained 94 % of its initial IEC and 93 % of its initial conductivtiy [15]. The PSF-0C0-ASD AEM displayed nearly 99 % conductivity retention after 1 M KOH treatment at 80 °C for 720 h [24]. The SEBSC6-MPy membrane exhibited the conductivity retention rate of 87.1 % after 600 h in 1 M KOH at 80 °C [32]. In addition, the chemical stability of AEMs in concentrated basic solutions is particularly appealing. As shown in Fig. S3, the rate of conductivity decay under a severe alkaline condition, i.e. in 10 mol/L aqueous KOH solution at 60 °C, was significantly higher than in the 1 mol/L aqueous KOH at 80 °C, especially for the Pip-C_{Bn}/PBI membrane. These results suggest that further optimization of the chemical structure of poly(bis-piperidinium) poly(ionic liquid)s is essential to meet the stringent requirements of high alkalinity environments.

The stability windows and degradation mechanisms of PBI in alkaline environment has recently been investigated in detail [62], and the rate of chain scission in 1 mol/L KOH at close to 90 °C is relatively low [63]. To assess the stability of the Pip-C_x component, Pip-C_4 and Pip-C_{Bn} were immersed in 1 mol/L NaOD/D_2O solution at 80 °C while collecting the ^{1}H NMR spectral evolution, as shown in Fig. 9a and b. For Pip-C_4, new peaks (star symbol) could not be observed in the ^{1}H NMR spectrum until 720 h in the test solution. The appearance of those new signals were probably due to the ring-opening of piperidinium cations, in good agreement with the degradation mechanisms reported for similar piperidinium based AEMs by Marino et al. [12] and Allushi et al. [39]. As to Pip-C_{Bn}, several new peaks appeared in its NMR spectrum only after 48 h test. Espiritu et al. [27] and Arges et al. [37] separately pointed out that the benzylic cations directly on the backbone may lead to the fracture of polymer backbone. In addition, the Pip-C_4/PBI membrane was selected to further evaluate the stability experiment in 8 mol/L KOH solution. It was found that the conductivity was gradually decreased, but still retained 80 % of the initial conductivity after 528 h. These results indicated that the main-chain type poly(bis-piperidinium) with alkyl linkage, especially with C_4 linkage, exhibited better alkaline stability than that containing the benzyl group.

The alkaline stability of piperidinium cations adhered with alkyl or benzyl group was further compared by DFT calculations according to the molecular orbital theory. As shown in Fig. 10, four piperidinium cations were designed, representing the repeat units of Pip-C_4 and Pip-C_{Bn}. It can be seen that the lowest unoccupied molecular orbital (LUMO) energy of PMPip was 0.574 eV, which was obviously higher than that of BenMPip (−1.092 eV). It is previously reported that cations with a higher LUMO energy are less prone to be attacked by OH^- [64,65]. Thus, LUMO energy results further confirmed that the piperidinium cation with an alkyl side chain exhibited a higher alkaline stability than the one with benzyl group. Ethyl containing piperidinium cations (i.e., PEMPip and BenEMPip) exhibited the same trend of LUMO energy results. Since the ring-opening reaction is regarded as the main degradation pathways for *N*-heterocyclic cations, the possible degradation mechanism of piperidinium cations was further studied by a theoretical approach on the nucleophilic process. Fig. 10(b) and (c) depict the energy barrier associated with a transition state based on the possible ring-opening pathways of piperidinium cations. Here, ΔE means the energy between TS and initial state, which need to be overcome by OH^-. A higher ΔE represents a higher energy barrier for the attack of piperidinium cations by OH^-. Whatever the ring-opening degradation mechanism depended on route I (methyl substitution) or route II (Hofmann β-hydrogen elimination), PEMPip displayed higher ΔE values than BenEMPip, demonstrating a better alkaline stability of PEMPip. These results are in agreement with the abovementioned experimental observations.

3.5. Performance of vanadium redox flow battery (VRFB)

The technical feasibility of the Pip-C_6/PBI membrane in electrochemical applications was demonstrated by performing the vanadium redox flow battery (VRFB). Fig. S4(A) shows the charge–discharge curves of batteries with Pip-C_6/PBI and Nafion 115 membranes at 100 mA cm^{-2}. It can be seen that the battery equipped with Pip-C_6/PBI showed the higher charge–discharge capacities than that with Nafion115, indicating the superior ability of restraining the crossover of vanadium ions of Pip-C_6/PBI [8,58]. Long-term cycle stabilities of VRFBs with Pip-C_6/PBI and Nafion 115 membranes at 100 mA cm^{-2} are depicted in Fig. S4(B). Coulombic efficiencies (CEs) of the battery with Pip-C_6/PBI were stable and equal to nearly 100 %. Meanwhile, the

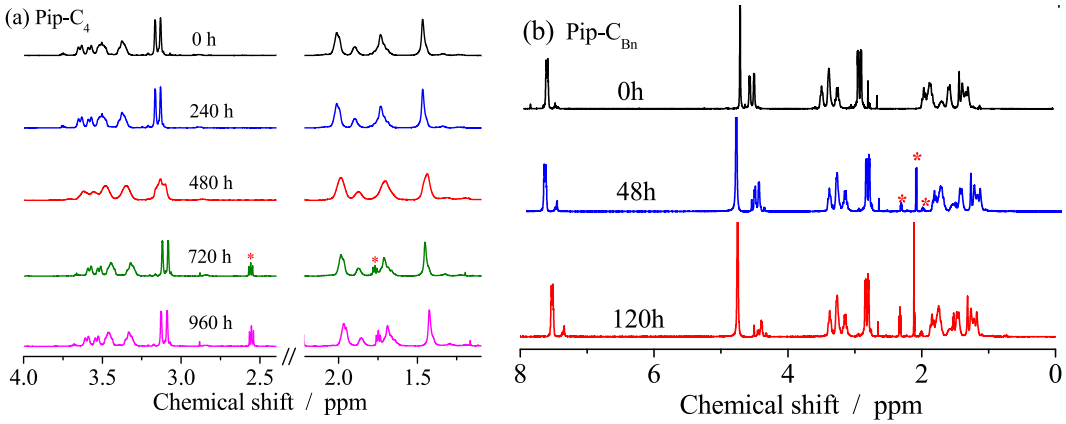

Fig. 9. ^{1}H NMR spectra (a and b) of Pip-C_4 and Pip-C_{Bn} when soaking in 1 mol/L NaOD/D_2O.

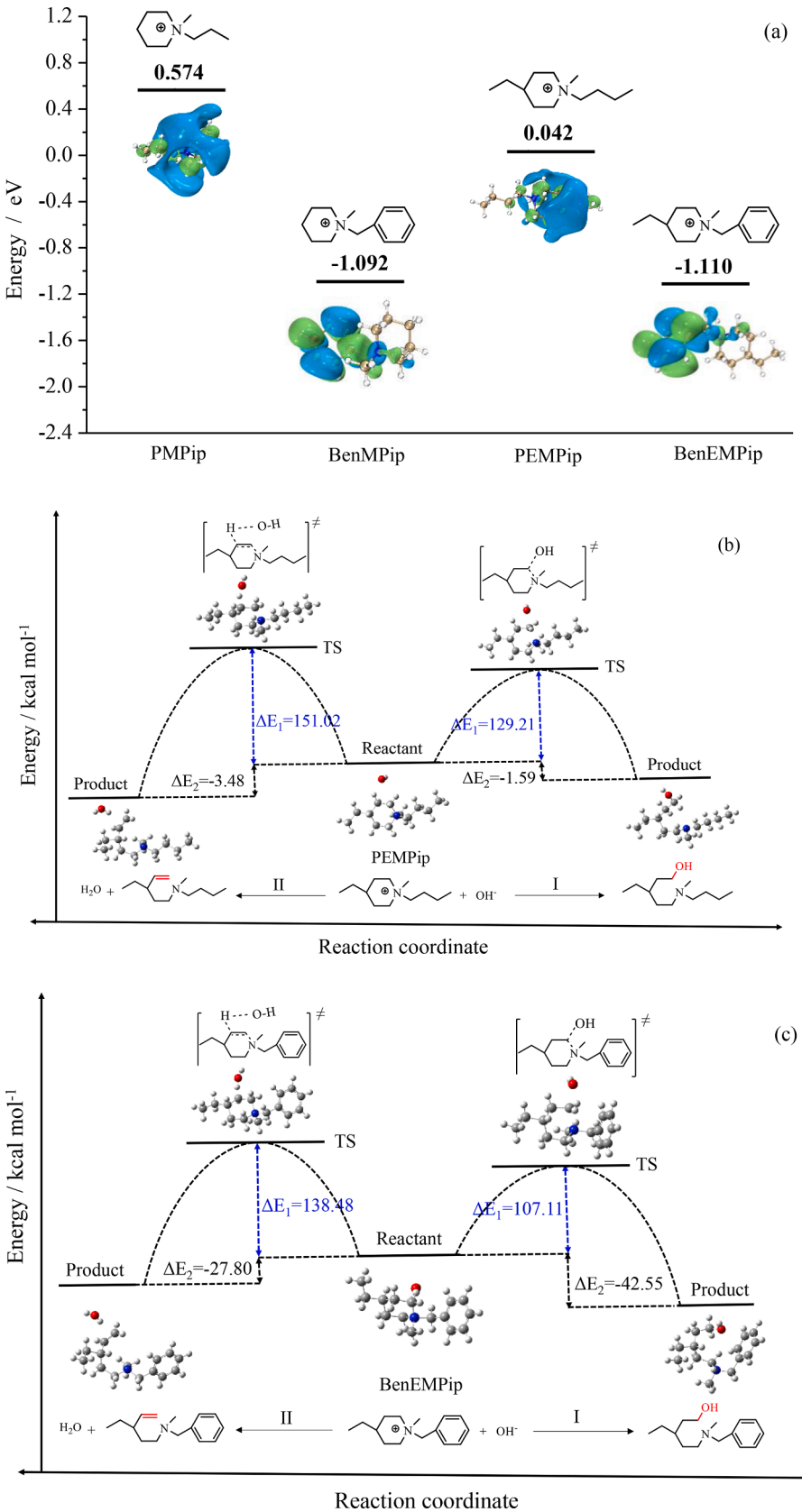

Fig. 10. (a) Frontier molecular orbital energy of various piperidinium cations; (b, c) possible degradation mechanism and reaction energy profiles for piperidinium cations under the attack of OH^-.

voltage efficiencies (VEs) and energy efficiencies (EEs) of the battery with Pip-C_6/PBI also remained stable values above 80 %, which were much higher than the battery with Nafion 115. The excellent VRFB performance of Pip-C_6/PBI was probably due to its lower vanadium ions permeation, which results from "Donnan exclusion effect", i.e. the repulsion effect of vanadium ions by the tethered positively charged groups. Therefore, the Pip-C_6/PBI membrane had a big potential for VRFB applications and other electrochemical devices [66,67].

4. Conclusions

A series of poly(ionic liquid)s of poly(bis-piperidinium)s were synthesized from the bis-piperidine monomer of TMBMP and seven bifunctional alkyl or aryl bromides. The Pip-C_{Bn} with the benzyl linkage reached the highest viscosity, while the inherent viscosity of the other poly(ionic liquid)s was increased as the increased length of aliphatic chains. ^{1}H NMR proved the successful synthesis of Pip-C_x poly(ionic liquid)s, which were subsequently blended with PBI to give mechanically robust and dimensionally stable AEMs. SEM images demonstrated the uniform and dense micromorphology of membranes. Among Pip-C_x/PBI membranes, Pip-C_{Bn}/PBI exhibited the highest water uptake and dimensional swellings. The chemical structure of spacer chain had a much more significant effect on the IEC and water uptake of Pip-C_x/PBI membranes comparing with temperature. As a result of the synergetic effect between water absorption and IEC on conductivity, the Pip-C_4/PBI membrane in Br^- form exhibited the highest conductivity of 67 mS cm^{-1} at 80 °C, when its IEC and WU% were 1.21 mmol g^{-1} and 50 %, respectively. Meanwhile, the mechanical strength and elongation of this membrane were around 13.4 MPa and 12.6 % at RT. As to alkaline stability, the Pip-C_4/PBI and Pip-C_6/PBI membranes maintained almost unchanged conductivities and IECs in 1 mol/L KOH at 60 °C during 1250 h. ^{1}H NMR confirmed Pip-C_{Bn} was easier to degrade in 1 mol/L NaOD/D_2O solution than Pip-C_4, which possible degradation mechanism was investigated by DTF. Furthermore, the Pip-C_4/PBI membrane retained 80 % of its initial conductivity in 8 M KOH at 80 °C after 528 h. Thus, this study provided a facile approach to design high-performance AEMs with superior alkaline stability.

CRediT authorship contribution statement

Beijia Zhao: Methodology, Writing – original draft, Writing – review & editing. **Tingting Wang:** Formal analysis, Investigation. **Mikkel Rykær Kraglund:** Investigation. **Jing Yang:** Investigation. **Jianhao Dong:** Investigation. **Ao Tang:** Investigation, Writing – original draft. **David Aili:** Funding acquisition, Writing – original draft, Writing – review & editing. **Jingshuai Yang:** Conceptualization, Funding acquisition, Supervision, Writing – original draft, Writing – review & editing.

Declaration of competing interest

The authors declare that they have no known competing financial interests or personal relationships that could have appeared to influence the work reported in this paper.

Data availability

Data will be made available on request.

Acknowledgements

The authors are grateful for the financial supports from the National Natural Science Foundation of China (51603031), Independent Research Fund Denmark (217-00074B), the Fundamental Research Funds for the Central Universities of China (N2005026), and the Liaoning Provincial Natural Science Foundation of China (2020-MS-087).

Appendix A. Supplementary data

Supplementary data to this article can be found online at https://doi.org/10.1016/j.molliq.2024.124775.

References

[1] R. Vinodh, R. Atchudan, H.J. Kim, M. Yi, Recent advancements in polysulfone based membranes for fuel cell (PEMFCs, DMFCs and AMFCs) applications: a critical review, Polymer 14 (2022) 300.
[2] W.E. Mustain, M. Chatenet, M. Page, Y.S. Kim, Durability challenges of anion exchange membrane fuel cells, Energy Environ. Sci. 13 (2020) 2805–2838.
[3] B.J. Zhao, Z.J. Zhang, J.W. Zhang, L. Wang, T.T. Wang, J.H. Dong, C.X. Xu, J. S. Yang, Long side-chain N-heterocyclic cation based ionic liquid grafted poly (terphenyl piperidinium) membranes for anion exchange membrane fuel cell applications, Polymer. 286 (2023) 126404.
[4] N.Y. Du, C. Roy, R. Peach, M. Turnbull, S. Thiele, C. Bock, Anion-exchange membrane water electrolyzers, Chem. Rev. 122 (2022) 11830–11895.
[5] C. Santoro, A. Lavacchi, P. Mustarelli, V. Di Noto, L. Elbaz, D.R. Dekel, F. Jaouen, What is next in anion-exchange membrane water electrolyzers? bottlenecks, benefits, and future, ChemSusChem 15 (2022) e202200027.
[6] H.H. Li, N. Yu, F. Gellrich, A.K. Reumert, M.R. Kraglund, J.H. Dong, D. Aili, J. S. Yang, Diamine crosslinked anion exchange membranes based on poly (vinylbenzyl methylpyrrolidinium) for alkaline water electrolysis, J. Membr. Sci. 633 (2021) 119418.
[7] C.A. Machado, G.O. Brown, R.D. Yang, T.E. Hopkins, J.G. Pribyl, T.H. Epps, Redox flow battery membranes: improving battery performance by leveraging structure-property relationships, ACS Energy Lett. 6 (2021) 158–176.
[8] X.F. Che, W.Q. Tang, J.H. Dong, D. Aili, J.S. Yang, Anion exchange membranes based on long side-chain quaternary ammonium-functionalized poly(arylene piperidinium)s for vanadium redox flow batteries, Sci. China-Mater. 65 (2022) 683–694.
[9] H. Feng, D. Liu, Y. Zhang, X.Y. Shi, O.C. Esan, Q. Li, R. Chen, L. An, Advances and challenges in photoelectrochemical redox batteries for solar energy conversion and storage, Adv. Energy Mater. 12 (2022) 2200469.
[10] N.J. Chen, Y.M. Lee, Anion-conducting polyelectrolytes for energy devices, Trends in Chem. 4 (2022) 236–249.
[11] J.R. Varcoe, P. Atanassov, D.R. Dekel, Dekel et al., Anion-exchange membranes in electrochemical energy systems, Energy Environ. Sci. 7 (2014) 3135–3191.
[12] M.G. Marino, K.D. Kreuer, Alkaline stability of quaternary ammonium cations for alkaline fuel cell membranes and ionic liquids, ChemSusChem 8 (2015) 513–523.
[13] S. Gottesfeld, D.R. Dekel, M. Page, C. Bae, Y. Yan, P. Zelenay, Y.S. Kim, Anion exchange membrane fuel cells: Current status and remaining challenges, J. Power Sources 375 (2018) 170–184.
[14] L. Zhu, X. Peng, S. Shang, M.T. Kwasny, T.J. Zimudzi, X. Yu, N. Saikia, J. Pan, Z. Liu, G.N. Tew, W.E. Mustain, M. Yandrasits, M.A. Hickner, High performance anion exchange membrane fuel cells enabled by fluoropoly(olefin) membranes, Adv. Funct. Mater. 29 (2019) 1902059.
[15] X. Wang, C. Lin, F. Liu, L. Li, Q. Yang, Q. Zhang, A. Zhu, Q. Liu, Alkali-stable partially fluorinated poly(arylene ether) anion exchange membranes with a claw-type head for fuel cells, J. Mater. Chem. A 6 (2018) 12455–12465.
[16] Y. Zhu, L. Ding, X. Liang, M.A. Shehzad, L. Wang, X. Ge, Y. He, L. Wu, J.R. Varcoe, T. Xu, Beneficial use of rotatable-spacer side-chains in alkaline anion exchange membranes for fuel cells, Energy Environ. Sci. 11 (2018) 3472–3479.
[17] J.S. Yang, C. Liu, Y.N. Hao, X.N. He, R.H. He, Preparation and investigation of various imidazolium-functionalized poly(2,6-dimethyl-1,4-phenylene oxide) anion exchange membranes, Electrochim. Acta 207 (2016) 112–119.
[18] S.H. Kim, K.H. Lee, J.Y. Chu, A.R. Kim, D.J.Y. Kim, Enhanced hydroxide conductivity and dimensional stability with blended membranes containing hyperbranched PAES/Linear PPO as anion exchange membranes, Polymers 12 (2020) 3011.
[19] R. Gokulapriyan, I. Arunkumar, H.K. Yoo, D.J. Yoo, Anion exchange membrane based on cross-linked poly(2,6-dimethyl-1,4-phenylene oxide)/poly (dimethylaminophenyl bisdiphenol) for fuel cell applications, ACS Appl. Energy Mater. 6 (2023) 12549–12559.
[20] K. Shen, Z. Zhang, H. Zhang, J. Pang, Z. Jiang, Poly(arylene ether ketone) carrying hyperquaternized pendants: Preparation, stability and conductivity, J. Power Sources 287 (2015) 439–447.
[21] B. Xue, X. Dong, Y. Li, J. Zheng, S. Li, S. Zhang, Synthesis of novel guanidinium-based anion-exchange membranes with controlled microblock structures, J. Membr. Sci. 537 (2017) 151–159.
[22] A.R. Kim, M.B. Poudel, J.Y. Chu, M. Vinothkannan, R.S. Kumar, N. Logeshwaran, B.H. Park, M.K. Han, D.J. Yoo, Advanced performance and ultra-high, long-term durability of acid-base blended membranes over 900 hours containing sulfonated PEEK and quaternized poly(arylene ether sulfone) in H2/O2 fuel cells, Compos. Pt. B-Eng 254 (2023) 110558.
[23] W. Chen, M. Hu, H. Wang, X. Wu, X. Gong, X. Yan, D. Zhen, G. He, Dimensionally stable hexamethylenetetramine functionalized polysulfone anion exchange membranes, J. Mater. Chem. A 5 (2017) 15038–15047.
[24] Y. Zhang, W.T. Chen, T.T. Li, X.M. Yan, F. Zhang, X.Z. Wang, X.M. Wu, B. Pang, G. H. He, A rod-coil grafts strategy for N-spirocyclic functionalized anion exchange membranes with high fuel cell power density, J. Power Sources 490 (2021) 229544.

[25] S. Chempath, B.R. Einsla, L.R. Pratt, C.S. Macomber, J.M. Boncella, J.A. Rau, B. S. Pivovar, Mechanism of tetraalkylammonium headgroup degradation in alkaline fuel cell membranes, J. Phys. Chem. C 112 (2008) 3179–3182.
[26] A.D. Mohanty, C. Bae, Mechanistic analysis of ammonium cation stability for alkaline exchange membrane fuel cells, J. Mater. Chem. A 2 (2014) 17314–17320.
[27] R. Espiritu, B.T. Golding, K. Scotta, M. Mamlouk, Degradation of radiation grafted anion exchange membranes tethered with different amine functional groups via removal of vinylbenzyl trimethylammonium hydroxide, J. Power Sources 375 (2018) 373–386.
[28] B. Lin, F. Xu, F. Chu, Y. Ren, J. Ding, F. Yan, Bis-imidazolium based poly(phenylene oxide) anion exchange membranes for fuel cells: the effect of cross-linking, J. Mater. Chem. A 7 (2019) 13275–13283.
[29] N. Yu, J.H. Dong, T.T. Wang, Y.P. Jin, W.Q. Tang, J.S. Yang, Two new anion exchange membranes based on poly(bis-arylimidazolium) ionenes blend polybenzimidazole, Polymer 240 (2022) 124491.
[30] J. Ponce-González, D.K. Whelligan, L. Wang, et al., High performance aliphatic-heterocyclic benzyl-quaternary ammonium radiation-grafted anion-exchange membranes, Energy Environ. Sci. 9 (2016) 3724–3735.
[31] H. Li, M.R. Kraglund, A.K. Reumert, X. Ren, D. Aili, J. Yang, Poly(vinyl benzyl methylpyrrolidinium) hydroxide derived anion exchange membranes for water electrolysis, J. Mater. Chem. A 7 (2019) 17914–17922.
[32] N. Yu, J.H. Dong, H.H. Li, T.T. Wang, J.S. Yang, Improving the performance of quaternized SEBS based anion exchange membranes by adjusting the functional group and side chain structure, Eur. Polym. J. 154 (2021) 110528.
[33] H.-S. Dang, P. Jannasch, Alkali-stable and highly anion conducting poly(phenylene oxide)s carrying quaternary piperidinium cations, J. Mater. Chem. A 4 (2016) 11924–11938.
[34] D. Yao, T. Wei, L. Shang, H. Na, C. Zhao, A comparative study of side-chain-type poly(ether ether ketone) anion exchange membrane functionalized with different hetero-cycloaliphatic quaternary ammonium groups, RSC Adv. 9 (2019) 7975–7983.
[35] R. Lv, S. Jin, L. Li, Q. Wang, L. Wang, J. Wang, J. Yang, The influence of comonomer structure on properties of poly(aromatic pyridine) copolymer membranes for HT-PEMFCs, J. Membr. Sci. 701 (2024) 122703.
[36] E.J. Park, S. Maurya, M.R. Hibbs, C.H. Fujimoto, K.-D. Kreuer, Y.S. Kim, Alkaline stability of quaternized Diels-Alder polyphenylenes, Macromolecules 52 (2019) 5419–5428.
[37] C.G. Arges, V. Ramani, Two-dimensional NMR spectroscopy reveals cation-triggered backbone degradation in polysulfone-based anion exchange membranes, Proc. Natl. Acad. Sci. u. s. a. 110 (2013) 2490–2495.
[38] S. Miyanishi, T. Yamaguchi, Ether cleavage-triggered degradation of benzyl alkylammonium cations for polyethersulfone anion exchange membranes, Phys. Chem. Chem. Phys. 18 (2016) 12009–12023.
[39] A. Allushi, T.H. Pham, J.S. Olsson, P. Jannasch, Ether-free polyfluorenes tethered with quinuclidinium cations as hydroxide exchange membranes, J. Mater. Chem. A 7 (2019) 27164–27174.
[40] R.E. Coppola, D. Herranz, R. Escudero-Cid, N. Ming, N.B. D'Accorso, P. Ocon, G. C. Abuin, Polybenzimidazole-crosslinked-poly(vinyl benzyl chloride) as anion exchange membrane for alkaline electrolyzers, Renew, Energ. 157 (2020) 71–82.
[41] K. Min, J.E. Chae, Y. Lee, H.J. Kim, T.H. Kim, Crosslinked poly(m-terphenyl N-methyl piperidinium)-SEBS membranes with aryl-ether free and kinked backbones as highly stable and conductive anion exchange membranes, J. Membr. Sci. 653 (2022) 120487.
[42] F.H. Wang, Y.H. Cui, J. Sang, H.F. Zhang, H. Zhu, Cross-linked of poly(biphenyl pyridine) and poly(styrene-b-(ethylene-co-butylene)-b-styrene) grafted with double cations for anion exchange membrane, Electrochim. Acta 405 (2022) 139770.
[43] F. Xu, K. Qiu, B. Lin, Y. Ren, J. Li, J. Ding, M.A. Hickner, Enhanced performance of poly(olefin)-based anion exchange membranes cross-linked by triallylmethyl ammonium iodine and divinylbenzene, J. Membr. Sci. 637 (2021) 119629.
[44] I. Strużyńska-Piron, M. Jung, A. Maljusch, O. Conradi, S. Kim, J.H. Jang, H.-J. Kim, Y. Kwon, S.W. Nam, D. Henkensmeier, Imidazole based ionenes, their blends with PBI-OO and applicability as membrane in a vanadium redox flow battery, Eur. Polym. J. 96 (2017) 383–392.
[45] J. Fan, A.G. Wright, B. Britton, T. Weissbach, J.G. Thomas, J. Skalski, T.J. Ward, S. H. Peckham, Cationic polyelectrolytes, stable in 10 M KOHaq at 100 °C, ACS Macro Lett. 6 (2017) 1089–1093.
[46] W. You, K.M. Hugar, G.W. Coates, Synthesis of alkaline anion exchange membranes with chemically stable imidazolium cations: unexpected cross-linked macrocycles from ring-fused ROMP monomers, Macromolecules 51 (2018) 3212–3218.
[47] B. Sana, A. Das, T. Jana, Cross-linked polybenzimidazoles as alkaline stable anion exchange membranes, ACS Appl. Energy Mater. 5 (2022) 3626–3637.
[48] T.H. Pham, J.S. Olsson, P. Jannasch, N-spirocyclic quaternary ammonium ionenes for anion-exchange membranes, J. Am. Chem. Soc. 139 (2017) 2888–2891.
[49] J.S. Olsson, T.H. Pham, P. Jannasch, Poly(arylene piperidinium) hydroxide ion exchange membranes: synthesis, alkaline stability, and conductivity, Adv. Funct. Mater. 28 (2018) 1702758.
[50] X. Qiao, X. Wang, S. Liu, Y. Shen, N. Li, The alkaline stability and fuel cell performance of poly(N-spirocyclic quaternary ammonium) ionenes as anion exchange membrane, J. Membr. Sci. 630 (2021) 119325.
[51] X. Tan, Z. Sun, J. Pan, J. Zhao, H. Cao, H. Zhu, F. Yan, Alkaline stable pyrrolidinium-type main-chain polymer: The synergetic effect between adjacent cations, J. Membr. Sci. 618 (2021) 118689.
[52] M.L. Guo, J. Fang, H.K. Xu, W. Xu, X.H. Li, C.H. Lu, K.Y. Lan, Kunyuan Li, Synthesis and characterization of novel anion exchange membranes based on imidazolium-type ionic liquid for alkaline fuel cells, J. Membr. Sci. 362 (2010) 97–104.
[53] W.J. Qian, J. Texter, F. Yan, Frontiers in poly(ionic liquid)s: syntheses and applications, Chem. Soc. Rev. 46 (2017) 1124–1159.
[54] X. Zhang, J.K. Zhou, R. Wei, W.F. Zhao, S.D. Sun, C.S. Zhao, Design of anion species/strength responsive membranes via in-situ cross-linked copolymerization of ionic liquids, J. Membr. Sci. 535 (2017) 158–167.
[55] J.H. Dong, N. Yu, X.F. Che, R.H. Liu, D. Aili, J.S. Yang, Cationic ether-free poly(bis-alkylimidazolium) ionene blend polybenzimidazole as anion exchange membranes, Polym. Chem. 11 (2020) 6037.
[56] J.S. Yang, L.N. Cleemann, T. Steenberg, C. Terkelsen, Q.F. Li, J.O. Jensen, H. A. Hjuler, N.J. Bjerrum, R.H. He, High molecular weight polybenzimidazole membranes for high temperature PEMFC, Fuel Cells 14 (2014) 7–15.
[57] X. Che, L. Wang, T. Wang, J. Dong, J. Yang, The effect of grafted alkyl side chains on the properties of poly(terphenyl piperidinium) based high temperature proton exchange membranes, Ind. Chem. Mater. 1 (2023) 516–525.
[58] X.R. Ren, L.N. Zhao, X.F. Che, Y.Y. Cai, Y.Q. Li, H.H. Li, H. Chen, H.X. He, J.G. Liu, J.S. Yang, Quaternary ammonium groups grafted polybenzimidazole membranes for vanadium redox flow battery applications, J. Power Sources 457 (2020) 228037.
[59] A. Zhegur-Khais, F. Kubannek, U. Krewer, D.R. Dekel, Measuring the true hydroxide conductivity of anion exchange membranes, J. Membr. Sci. 612 (2020) 118461.
[60] X.Z. Cao, D. Novitski, S. Holdcroft, Visualization of hydroxide ion formation upon electrolytic water splitting in an anion exchange membrane, ACS Mater. Lett. 1 (2019) 362–366.
[61] K.M. Meek, S. Sharick, Y.S. Ye, K.I. Winey, Y.A. Elabd, Bromide and hydroxide conductivity-morphology relationships in polymerized ionic liquid block copolymers, Macromolecules 48 (2015) 4850–4862.
[62] D. Serhiichuk, T. Patniboon, Y.F. Xia, M.R. Kraglund, J.O. Jensen, H.A. Hansen, D. Aili, Insight into the alkaline stability of arylene-Linked bis-benzimidazoles and polybenzimidazoles, ACS Appl. Polym. Mater. 5 (2023) 803–814.
[63] D. Aili, K. Jankova, Q.F. Li, N.J. Bjerrum, J.O. Jensen, The stability of poly(2,2 '-(m-phenylene)-5,5 '-bibenzimidazole) membranes in aqueous potassium hydroxide, J. Membr. Sci. 492 (2015) 422–429.
[64] W.B. Wang, G.B. Hammond, B. Xu, Ligand effects and ligand design in homogeneous gold(I) catalysis, J. Am. Chem. Soc. 134 (2012) 5697–5705.
[65] Z. Sun, J. Pan, J.N. Guo, F. Yan, The alkaline stability of anion exchange membrane for fuel cell applications: the effects of alkaline media, Adv. Sci. 5 (2018) 1800065.
[66] W.-F. Xie, M.-F. Shao, Alkaline water electrolysis for efficient hydrogen production, J. Electrochem. 28 (2022) 2214008.
[67] X.-R. Yun, Y.-F. Chen, P.-T. Xiao, C.-M. Zheng, Review on oxygen-free vanadium-based cathodes for aqueous zinc-ion batteries, J. Electrochem. 28 (2022) 2219004.